Article

Soluplus−TPGS Mixed Micelles as a Delivery System for Brigatinib: Characterization and In Vitro Evaluation

Raisuddin Ali, Wajhul Qamar, Mohd Abul Kalam, and Ziyad Binkhathlan*

Read Online

ACCESS | Metrics & More | Article Recommendations

ABSTRACT: Lung cancer is a major public health concern, with a high incidence and fatality rate. Its treatment is very difficult, as it is mostly diagnosed in advanced stages. Non-small cell lung carcinoma (NSCLC) is the major form of lung carcinoma that persists. Brigatinib (BGT), a powerful small-molecule tyrosine kinase inhibitor, has demonstrated significant therapeutic potential in the treatment of NSCLC with anaplastic lymphoma kinase (ALK) mutations. However, the therapeutic applicability of BGT is hampered by its low solubility and bioavailability. In this study, we developed a mixed micelle system comprising Soluplus and TPGS loaded with BGT. BGT was encapsulated into the mixed micelles using various combinations of Soluplus and TPGS, with encapsulation efficiency (EE%) ranging from 52.43 ± 1.07 to $97.88 \pm 2.25\%$. The dynamic light scattering data showed that the mixed micelles ranged in size from 75.7 ± 0.46 to 204.3 ± 5.40 nm. The selected mixed micelles (F6) showed approximately 38% BGT release in the first 2 h, and subsequently, within 72 h, the release was $94.50 \pm 5.90\%$. The NMR experiment confirmed the formation of micelles. Additionally, the mixed micelles showed significantly higher cellular uptake ($p < 0.05$) and increased cytotoxicity ($p < 0.05$) as compared to the free BGT. Specifically, the obtained IC_{50} values for BGT-loaded Soluplus−TPGS mixed micelles and free BGT were 22.59 ± 6.07 and 61.45 ± 6.35 $\mu g/mL$, respectively. The results of the in vitro stability experiment showed that the selected mixed micelle (F6) was stable at both room temperature and 4 °C, with only minor changes in size and PDI. Our results indicate great potential for the developed Soluplus−TPGS mixed micelles as a delivery system for BGT.
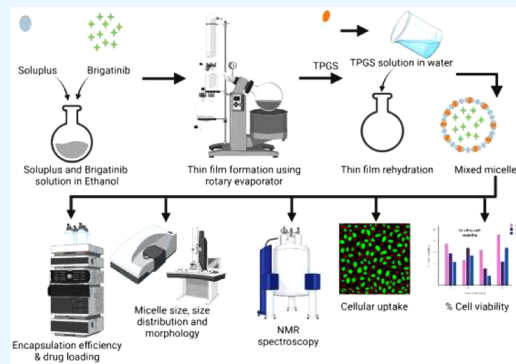
1. INTRODUCTION

Cancer is a condition characterized by an uncontrolled division of aberrant cells that can spread from one organ to another or different regions of the body. It starts with a genetic mutation of a single cell that allows it to divide and multiply uncontrollably. These mutations are either inherited or acquired.[1] The acquired mutation can be caused by environmental exposures such as ultraviolet rays or smoking. Out of the different types of cancer, lung cancer is a major public health concern, with a high incidence and fatality rate. It is the second most prevalent cancer worldwide. According to GLOBOCAN 2020 cancer incidences and mortality estimates, lung cancer has become the second most diagnosed (11.4%) cancer and the leading cause of cancer death (18%) worldwide.[2] The lung cancer is lethal because it initially shows no signs or symptoms and is only identified in its advanced stages. The incidence of lung cancer is higher among males compared to females.[3] It must be promptly diagnosed and staged (size of the tumor and its extent) for a better prognosis.

Lung cancer is classified into two major groups, non-small cell lung carcinoma (NSCLC) and small cell lung carcinoma (SCLC). NSCLC is the most common form of lung cancer.[4]

Depending on the stage of NSCLC, the main treatment options include surgery, radio frequency ablation, radiation therapy, chemotherapy, targeted medication therapy, immunotherapy, and palliative procedures. With the advancement of molecular and diagnostic procedures, the researchers have gained insights into the etiology of NSCLC and identified their genomic biomarkers. These biomarkers include Kirsten rat sarcoma viral oncogene homologue (KRAS), epidermal growth factor receptor (EGFR), anaplastic lymphoma kinase (ALK), ROS proto oncogene 1 (ROS1), B-RAF proto oncogene (BRAF), RET proto oncogene (RET), MET proto oncogene (MET), human epidermal growth factor receptor 2 (HER2), and neurotrophic receptor tyrosine kinase (NTRK).[5] The knowledge of these biomarkers helped in the development of the drugs that precisely target these oncogenic mutations.

A

Brigatinib (BGT), a potent small-molecule tyrosine kinase inhibitor, has shown remarkable therapeutic potential in the treatment of NSCLC with ALK mutations. It received FDA approval in 2017 for the treatment of NSCLC. BGT is considered a breakthrough drug because it has successfully addressed the issue of drug resistance associated with the first-generation oral tyrosine kinase ALK inhibitor (Crizotinib) and second-generation tyrosine kinase ALK inhibitors (Ceritinib and Alectinib). It effectively inhibits both trans-membrane proteins, EGFR and ALK in humans.[6] The superior inhibitory effects of BGT against NSCLC with ALK mutations are primarily due to the specific affinity of its dimethyl phosphine oxide moiety to the ALK.[7] However, the clinical application of BGT is hindered by its poor solubility and limited bioavailability.[8] Specifically, the reported aqueous solubility of BGT is around 0.1 mg/mL.[9] Although the exact absolute bioavailability of BGT in humans remains unknown due to the lack of pharmacokinetic data following intravenous administration, it was estimated to be 46%,[10] which is within the range reported in rat and monkey (40−53%).[11] In addition to its low solubility, BGT is a substrate for the CYP3A enzyme, P-glycoprotein (P-gp), and breast cancer resistance protein (BCRP).[10] These factors likely contribute to its low bioavailability due to the first-pass effect and intestinal efflux.

Nanotechnology has emerged as a promising field in medical research and treatment, offering innovative solutions for diagnosing, treating, and preventing various ailments. Liposomes,[12] solid lipid nanoparticles,[13] and polymeric nanoparticles[14] are some of the nanotechnology-based formulations that enhance the properties and effectiveness of pharmaceutical products. In order to address the challenges associated with BGT delivery, researchers have turned to nanotechnology-based drug delivery systems, including nanospanlastics,[15] solid lipid nanoparticles,[16] self-nanoemulsifying drug delivery systems,[17] and polymeric nanoparticles.[18] Polymeric micelles have attracted attention in drug delivery due to their biocompatibility, core−shell structure that protects active molecules in their core, low toxicity, stable morphology, and nanoscale size. Polymeric micelles can also address the solubility issue of hydrophobic drugs.[19] Recently, "mixed micelles" systems have been introduced to utilize the properties of two or more block copolymers to improve the qualities of the single micelle system.[20] These include improved kinetic and thermodynamic stability, more precise control over size, increased drug loading capacities, and easy surface modification.[21] The mixed micelle system may lower reticuloendothelial system uptake, as well as improve drug targeting by increasing permeability and retention.[22] Furthermore, mixed micelles have a size range of 20 to 200 nm, which is sufficient to avoid quick clearance from renal tubules yet small enough to permeate through capillaries in order to improve targeting and limit off-target toxicity. Thus, mixed micelles can minimize the negative effects of anticancer medications.[23]

Polyvinyl caprolactam-polyvinyl acetate-polyethylene glycol graft copolymer (Soluplus) is a novel amphiphilic polymer that has been shown to improve the solubility of numerous hydrophobic medicines such as acyclovir,[24] scopoletin,[25] febendazole,[26] and cyclosporine A.[27] Soluplus has reportedly a very low critical micellar concentration (CMC) value of around 7.6 μg/mL and a high hydrophilic lipophilic balance (HLB) value of approximately 14. This combination provides high stability to the micelles against dilution.[28]

D-α-tocopheryl polyethylene glycol 1000 succinate (TPGS) is a biomaterial that has been commonly used for the preparation of mixed micelles. TPGS is an FDA-approved, synthetic and water-soluble derivative of vitamin E and composed of both hydrophilic (PEG chain) and hydrophobic (vitamin E) parts.[29] TPGS is mainly used as a surfactant, solubilizing agent, and permeation enhancer for hydrophobic drugs.[30] TPGS also acts as a P-gp inhibitor and helps in overcoming multi-drug resistance (MDR) in cancer treatments.[31]

In the current work, BGT was encapsulated in the mixed micellar system based on Soluplus and TPGS, in order to enhance its aqueous solubility and improve the in vitro antitumor activity. The physicochemical properties of the BGT-loaded mixed micelles, such as percentage drug loading (DL%), encapsulation efficiency (EE%), particle size, polydispersity (PDI), morphology, in vitro stability, and in vitro release profile, were investigated. Finally, in vitro cellular uptake and cytotoxicity in human lung cancer cell lines (A549) were also studied.

2. RESULTS AND DISCUSSION

2.1. Preparation of BGT-Loaded Single and Mixed Micelles.
The present investigation utilizes amphiphilic copolymers, Soluplus and TPGS in various combinations to generate mixed micelles as prospective nanocarriers for BGT delivery. Soluplus is an amphiphilic graft copolymer of vinyl caprolactam: vinyl acetate: polyethylene glycol 6000 (57:30:13) and reportedly increased the solubility of various hydrophobic drugs.[32] TPGS is an FDA-approved amphiphilic polymer with wide range of applications such as good biocompatibility, penetration enhancer, augmentation of solubility, P-gp inhibition, and specific antitumor activity.[33] With the aim of utilizing the benefits of both polymers for BGT delivery, the mixed micelles were prepared. Ethanol has been reported to produce mixed micelles using Soluplus and TPGS. Additionally, BGT is sufficiently soluble in ethanol.[9] Ethanol was chosen as the solvent due to its classification as a class 3 residual solvent, which is considered less toxic compared to class 1 and 2 solvents.[34]

2.2. CMC Determination.
The minimum polymer concentration that sufficiently reduces the interfacial energies to allow micelle formation is known as the CMC. The CMC is equally important for mixed micelles as it is for single-component micelles. Mixed micelles are formed when two or more different types of surfactant molecules and/or amphiphilic polymers are present in a solution. These surfactants can have different chemical structures and properties, and their interactions can significantly affect the behavior of the mixed micelles. CMC aids in establishing the concentration at which these mixed systems become efficient and stable, making them useful in a variety of applications ranging from drug delivery to industrial operations.[35]

Dynamic light scattering (DLS) is an effective method for calculating the CMC. DLS can provide valuable insights into the production of micelles and the transition from individual molecules to micellar aggregates. As surfactant concentration approaches the CMC during micelle formation, a sudden increase in the intensity of scattered light occurs due to changes in particle size and polydispersity.[36] The DLS technique measures the intensity of light scattered by a sample as a function of angle θ with respect to the direction of the incident light beam and provides results as derived count rates.

Table 1 shows the CMC results of the Soluplus/TPGS single and mixed micelles. The CMC of Soluplus and TPGS was

Table 1. CMC Values of Different Micellar Systems in Water at 25 °C[a]

Code	Soluplus: TPGS	CMC (μg/mL)
B1	0:5	604.35 ± 21.60
B2	1:4	251.30 ± 5.80[bc]
B3	2:3	220.90 ± 7.73[bc]
B4	1:1	184.28 ± 2.18[bc]
B5	3:2	161.43 ± 11.18[c]
B6	4:1	116.54 ± 0.61[bc]
B7	5:0	36.38 ± 0.83[b]

[a]Data are presented as mean ± SD ($n = 3$). [b]Significantly different from the CMC of TPGS. [c]Significantly different from the CMC of Soluplus.

found to be 36.38 ± 0.83 and 604.35 ± 21.60 μg/mL, respectively. The CMC of mixed micellar system was observed to be in the range of 116.54 ± 0.61 to 251.30 ± 5.80 μg/mL. A very intriguing relationship was discovered between the CMC values of various Soluplus: TPGS proportions. The experimental CMC values increased with the higher proportions of TPGS in the mixed micellar system. Similar observations were reported by Cagel et al.[37] The higher TPGS content has a negative influence on self-aggregation behavior of Soluplus.[28] This impact is most likely explained on the basis of reduced hydrophobic interactions between the core forming blocks of Soluplus and Vitamin E segment of TPGS at the micellar core.[28] Similarly, the comparison of the CMC of different mixed micellar systems studied is always lower than that of TPGS single micelles. This indicates that mixed micelles are comparatively more thermodynamically stable than TPGS single micelles. Thus, the incorporation of Soluplus and TPGS in the preparation of mixed micelles has an overall positive impact, which can improve the stability of the mixed micelles.

2.3. Measurement of Micellar Size, Polydispersity Index (PDI), and Zeta Potential. The single and mixed micelles were successfully prepared by a thin film hydration method. The mean diameter of blank single micelles of TPGS and Soluplus was found to be 13.16 ± 1.07 and 65.72 ± 1.40 nm, respectively, whereas the blank mixed micelles were found to be in the range of 62.46 ± 2.08 to 192.26 ± 1.11 nm with a unimodal size distribution (Table 2). An increase in mean micelle size is observed when the percentage composition of TPGS increased from 20 to 80%. Similar behavior was reported by Bernabeu et al.[28] The insertion of TPGS chains in the shell and core of Soluplus-based micelles during micellization may be responsible for the change in the size of mixed micelles. The mean diameters of BGT-loaded Soluplus and TPGS micelles were found to be 71.92 ± 1.39 and 24.39 ± 1.98 nm, respectively (Table 2). An intriguing behavior was seen with BGT-loaded mixed micelles containing a larger amount of TPGS. The BGT-loaded micelles with higher TPGS content (F2, F3, and F4) showed bimodal particle size distribution as shown in Table 2. The smaller and larger particles were in the range of 14.3 ± 0.44 to 24.39 ± 1.98 nm and 163.73 ± 6.64 to 204.27 ± 5.40 nm, respectively. The possible explanation of the bimodal size distribution is the presence of excess TPGS, which is not utilized completely during the formation of mixed micelles and single micelles of TPGS were also formed. When the TPGS content was reduced from 80% to 50%, the percentage of smaller particles decreased from 58.5% to 16.83%, corroborating the hypothesis. The BGT-loaded mixed micelles with higher Soluplus content (F5 and F6) showed unimodal particle size distribution having mean diameters of 134.88 ± 2.48 and 75.7 ± 0.46, respectively. The PDI values for blank single micelles were 0.023 ± 0.005 (TPGS) and 0.069 ± 0.014 (Soluplus), while BGT-loaded single micelles showed PDI values of 0.027 ± 0.007 (TPGS) and 0.089 ± 0.011 (Soluplus). The blank mixed micelles had PDI relatively lower than that of their BGT-loaded counterparts (Table 2) except for formulation F6. The PDI values of

Table 2. Particle size, distribution, and zeta potential of blank and BGT-loaded micellar systems[a]

Formulation code	Soluplus: TPGS	Particle sizes				PDI	Zeta potential (mV)
		Peak 1		Peak 2			
		D (nm)	%	D (nm)	%		
		Blank Micelles					
B1	0:5	13.16 ± 1.07	100.00	–	–	0.023 ± 0.005	−2.30 ± 1.2
B2	1:4	192.26 ± 1.11	100.00	–	–	0.292 ± 0.070	−2.08 ± 0.4
B3	2:3	162.73 ± 3.70	100.00	–	–	0.223 ± 0.035	−2.18 ± 0.1
B4	1:1	127.53 ± 5.80	100.00	–	–	0.230 ± 0.039	−1.48 ± 0.2
B5	3:2	126.63 ± 8.04	100.00	–	–	0.199 ± 0.011	−0.88 ± 0.1
B6	4:1	62.46 ± 2.08	100.00	–	–	0.137 ± 0.008	−0.81 ± 0.3
B7	5:0	65.72 ± 1.40	100.00	–	–	0.069 ± 0.014	−0.19 ± 0.1
		BGT-Loaded Micelles					
F1	0:05	24.39 ± 1.98[b]	100.00	–	–	0.027 ± 0.007	−4.68 ± 0.4
F2	1:4	25.58 ± 2.56	58.50	204.27 ± 5.40[b]	41.50	0.364 ± 0.006	−2.10 ± 0.3
F3	2:3	14.97 ± 0.33	58.26	175.92 ± 7.51	41.74	0.402 ± 0.033[c]	−2.15 ± 0.2
F4	1:1	14.3 ± 0.44	16.83	163.73 ± 6.64[b]	83.17	0.472 ± 0.050[c]	−2.54 ± 0.3
F5	3:2	134.88 ± 2.48[b]	100.00	–	–	0.171 ± 0.003[c]	−1.10 ± 0.5
F6	4:1	75.7 ± 0.46[b]	100.00	–	–	0.056 ± 0.012[c]	−0.91 ± 0.1
F7	5:1	71.92 ± 1.39	100.00	–	–	0.089 ± 0.011	−1.21 ± 0.3

[a]Data are presented as mean ± SD ($n = 3$). [b]Particle size significantly different from their blank equivalent ($p < 0.05$; paired Student's t test) in Table 2. [c]PDI significantly different from their blank equivalent ($p < 0.05$; paired Student's t test) in Table 2.
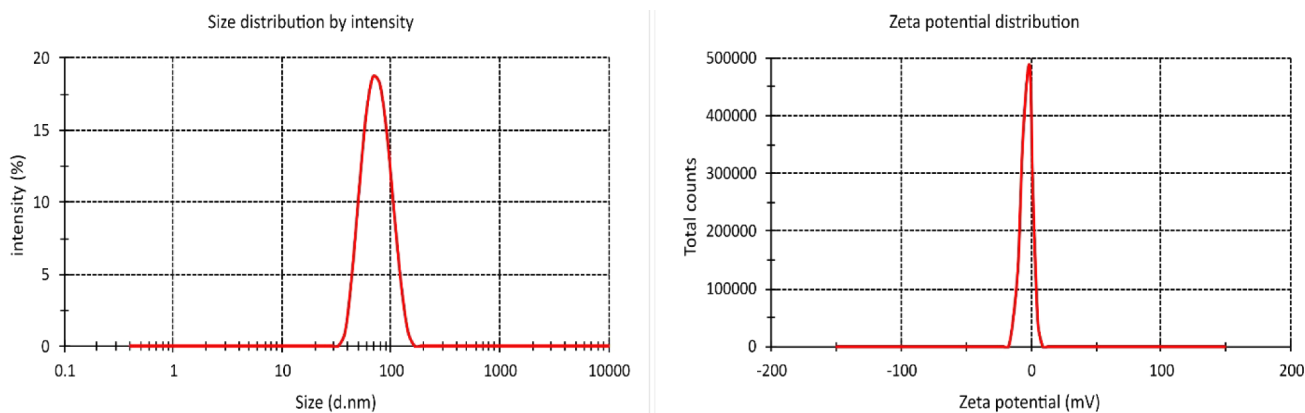
Figure 1. Size and zeta potential distribution of the BGT-loaded Soluplus/TPGS mixed micelle (F6).

micelles F2, F3, and F4 were very high owing to their bimodal size distribution.

The zeta potential of blank micelles ranged from -2.30 ± 1.2 to -0.19 ± 0.1 mV, whereas BGT-loaded micelles had zeta potential values in the range of -4.68 ± 0.4 to -0.91 ± 0.1 mV (Table 2). Soluplus and TPGS are nonionic amphiphilic polymers having PEG chains as the hydrophilic domain. PEG chains are responsible for the formation of the shell during self-assembly to form micelles. This shell imparts stability to the micelles in water. Overall, PEG acts as a steric stabilizer, and sterically stable systems have restricted zeta potential application. Despite having a zeta potential values that are nearly neutral, these systems remain stable.[38] Representative size and zeta potential distribution curve for formulation F6 are presented in Figure 1.

2.4. Estimation of Encapsulation Efficiency (EE%) and Drug Loading (DL%). The encapsulation of drugs inside the micellar core is mainly dependent upon their affinities and compatibility. The encapsulation increases if the drug has more compatibility and affinity for the micellar core, and vice versa.[39] In the current work, single micelles prepared from Soluplus ($95.37 \pm 2.28\%$) demonstrated considerably higher encapsulation efficiency ($p < 0.05$) as compared those prepared from TPGS ($34.3 \pm 21.27\%$) alone, demonstrating that BGT has a stronger affinity for the core-forming block of Soluplus. Table 3 shows the EE% and DL% of the single and mixed micelles.

The EE% and DL% of the mixed micelles increased when Soluplus content increased from 20% (Soluplus: TPGS 1:4) to 60% (Soluplus: TPGS 3:2). Further increment in the Soluplus proportion had no discernible effect on the EE%, and Formulation F5 (Soluplus: TPGS 3:2) and F6 (Soluplus: TPGS 4:1) have comparable EE%. The EE% of F5 and F6

were found to be 97.88 ± 2.25 and 96.21 ± 1.44 respectively. This %EE value translates to a drug solubility of 0.978 mg/mL, which is around 10-times higher than the aqueous solubility reported for BGT.[9] A similar pattern was seen for the DL% of different formulations. The DL% of mixed micelles F2, F3, F4, and F5 was in the order of F2 < F3 < F4 < F5, whereas the DL% of formulations F5 and F6 was identical. All Soluplus: TPGS ratios employed to prepare mixed micelles, as well as Soluplus and TPGS single micelles, clearly increased the BGT solubility as compared to free BGT. Another critical matter to consider is the impact of TPGS proportion on the EE% and DL%. As shown in Table 3, increasing the amount of TPGS in the mixed micelles had a negative effect on BGT encapsulation. As a result, the EE% of BGT was significantly lower for formulations F2, F3, and F4 ($p < 0.05$) compared to that obtained with Soluplus single micelles. As previously discussed in section 2.2, reduced hydrophobic interactions in the core building blocks of Soluplus and TPGS may account for the negative microenvironment for the encapsulation of BGT, which resulted in a lower EE% of mixed micelles with higher TPGS proportions. It has been previously reported that the hydrophobic characteristic of the micellar core substantially increases the solubility hydrophobic drugs via hydrophobic–hydrophobic interactions.[40]

2.5. In Vitro Release Profile of BGT from Mixed Micelles. The in vitro release experiments of BGT from single and mixed micelles were performed at pH 7.4 and compared with the BGT ethanolic solution, which served as a control. Figure 2 represents the in vitro release profile of BGT from ethanolic solution, formulations F5, F6, and F7 in phosphate-buffered saline (pH 7.4) containing 0.5% v/v Tween 80. Within 9 h, the ethanolic solution released roughly $98.5 \pm 3.52\%$, while F7 released $85.75 \pm 4.76\%$ BGT. For the ethanolic solution and F7, the 100% release was attained in 12 and 24 h, respectively. On the contrary, mixed micelles F5 and F6 demonstrated biphasic release behavior (Figure 2). The BGT release from formulations F5 and F6 was approximately 38% in the first 2 h. Over the next 22 h, the BGT release increased steadily to $80.30 \pm 3.21\%$ and $85.65 \pm 3.90\%$, for formulations F5 and F6, respectively. Subsequently, both formulations demonstrated slow release up to 72 h, and the maximum release achieved was $83.15 \pm 3.96\%$ for F5 and $94.50 \pm 5.90\%$ for F6. The control group's complete release demonstrates that the experimental design was valid. The release experiment for mixed micelles having the maximum level of TPGS (F2) was also carried out (data not shown), and
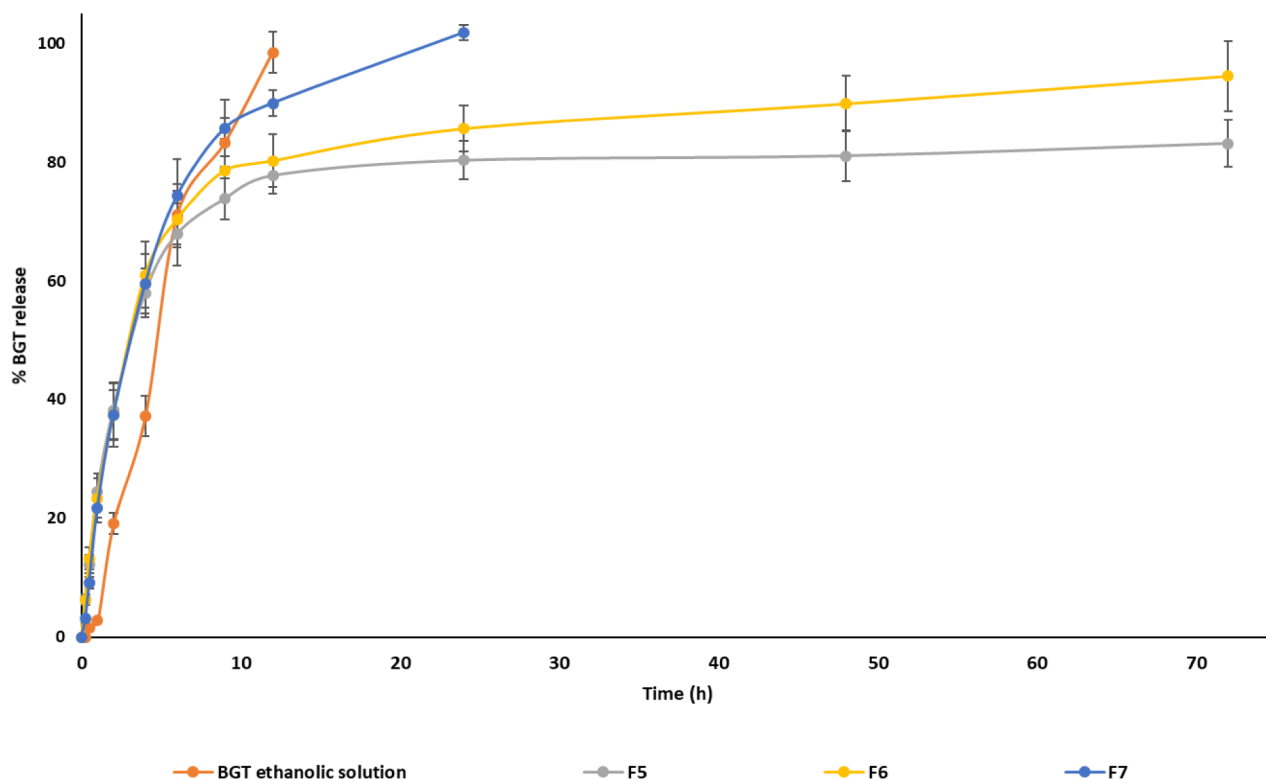
Table 3. Encapsulation Efficiency (EE%) and Percentage Drug Loading (DL%) of Different Mixed Micelles[a]

Formulation code	%EE	%DL
F1	34.32 ± 1.27	2.02 ± 0.08
F2	52.43 ± 1.07^{bc}	3.08 ± 0.12^{de}
F3	69.32 ± 1.33^{bc}	4.08 ± 0.08^{de}
F4	72.92 ± 1.05^{bc}	4.29 ± 0.10^{de}
F5	97.88 ± 2.25^{b}	5.76 ± 0.14^{d}
F6	96.21 ± 1.44^{b}	5.66 ± 0.09^{d}
F7	95.37 ± 2.28^{b}	5.61 ± 0.14^{d}

[a]Data are presented as mean $\pm$ SD ($n = 3$). [b]$p < 0.05$ versus F1. [c]$p < 0.05$ versus F7. [d]$p < 0.05$ versus F1. [e]$p < 0.05$ versus F7.

Figure 2. In vitro release profile of BGT ethanolic solution, F5, F6, and F7 in phosphate-buffered saline (PBS, pH = 7.4) containing 0.5% v/v Tween 80 at 37 °C temperature.

Table 4. Mathematical Models and Their Equations Used to Describe the Release

Model	Equation	Parameter	R^2 Adjusted	AIC[a]	MSC[b]
Zero order	$F = k_0 t$	k_0 1.871	−0.7706	110.13	−0.75
First order	$F = 100(1 - e^{-k_1 t})$	k_1 0.049	0.202	71.41	2.76
Higuchi	$F = k_H t^{1/2}$	k_H 15.339	0.4505	97.26	0.42
Korsmeyer-Peppas	$F = k_{KP} t^n$	k_{KP} 35.152, n 0.262	0.8163	86.05	1.44
Hixson-Crowell	$F = 100[1 - (1 - k_{HC} t)^3]$	k_{HC} 0.022	0.4527	97.22	0.42
Peppas-Sahlin	$F = k_1 t^m + k_2 t^{2m}$	k_1 32.03, k_2 −2.60, m 0.490	0.9351	75.31	2.41
Quadratic	$F = 100(k_1 t^2 + k_2 t)$	k_1 −0.001, k_2 0.058	0.2146	102.03	−0.02
Weibull	$F = 100\{1 - e^{-[(t - t_i)^\beta]/\alpha}\}$	α 2.693, β 0.605, t_i −0.218	0.9736	65.41	3.31

[a]AIC Akaike information criterion. [b]MSC model selection criterion.

it was discovered that F2 and likewise F7 totally released BGT within 24 h.

The release data for formulation F6 was fitted with various release models using the DD solver MS Excel add-in application. The Weibull model was the best-fitting release kinetics model for formulation F6, with R^2 adjusted = 0.9736, an Akaike information criterion (AIC) value of 65.41, and a model selection criterion value of 3.31 (Table 4). The obtained β-value (0.605) for Weibull model supports the Fickian diffusion mechanism.[41] Based on the in vitro release data and physicochemical characterization (comparable EE% and smaller unimodal size distribution) of the mixed micelles, we chose the F6 formulation (Soluplus: TPGS ≡ 4:1) for the remaining studies (TEM imaging, in vitro cytotoxicity, and cellular uptake assays).

2.6. Morphological Examination. The morphology of blank (B6) and mixed micelle (F6) samples was examined by using a transmission electron microscope (TEM). The TEM images confirmed the selected micelles were spherical in shape with narrow size distribution (Figure 3). TEM images revealed
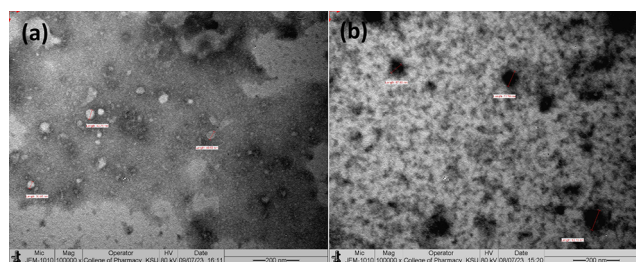

Figure 3. Representative TEM photographs of (a) blank mixed micelles B6 and (b) BGT-loaded mixed micelles F6 captured using JEOL JEM-1010 transmission electron microscope at 80 kV operating voltage.

that blank (B6) and BGT-loaded mixed micelles (F6) had average diameters of 43.61 ± 7.11 and 65.39 ± 8.20 nm, respectively. There were minor differences observed between the average size measurements of TEM and the Malvern particle size analysis. This difference could be explained by the fact that the Malvern particle size analyzer measures hydro-
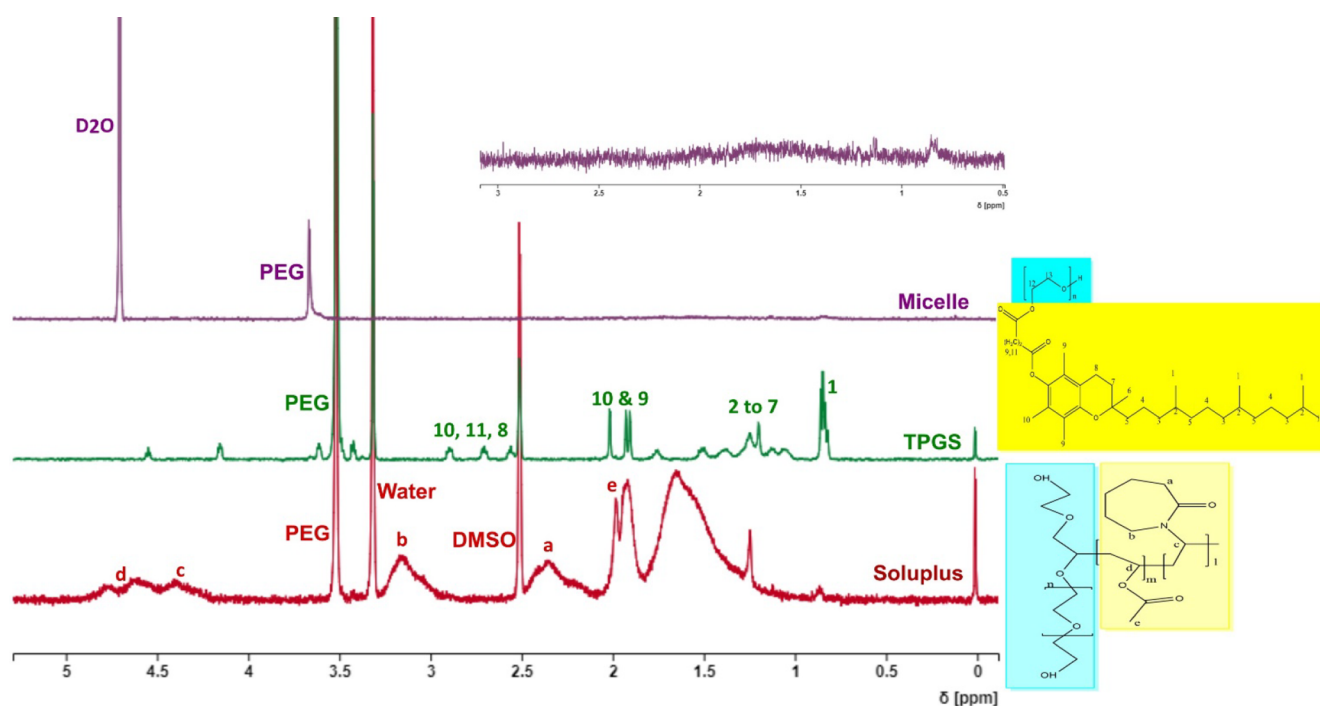
Figure 4. NMR spectra of Soluplus, TPGS, and B6 mixed micelles.

Table 5. Characteristics of Optimal BGT Loaded Mixed Micelles Upon Storage for 0, 5, 10, and 15 Days at Room Temperature and 4 °C[a]

		RT			REF		
	Day 0	Day 5	Day 10	Day 15	Day 5	Day 10	Day 15
Diameter (nm)	75.7 ± 0.46	77.1 ± 1.32	74.6 ± 0.90	76.3 ± 0.77	78.6 ± 2.14	79.3 ± 2.91	78.1 ± 3.02
PDI	0.056 ± 0.01	0.049 ± 0.02	0.050 ± 0.03	0.042 ± 0.03	0.07 ± 0.04	0.064 ± 0.05	0.055 ± 0.02
Zeta potential mV)	−0.91 ± 0.10	−1.10 ± 0.30*	−1.18 ± 0.27**	−1.23 ± 0.34**	−1.18 ± 0.27*	−1.10 ± 0.32*	−1.37 ± 0.39**
%EE	96.21 ± 1.44	95.86±2.38	96.35 ± 1.24	95.41 ± 2.10	96.11 ± 1.64	95.84 ± 2.18	95.21 ± 3.24

[a]Data are presented as mean ± SD (n = 3). * and ** Significantly different from the day 0 zeta potential values (p < 0.05; Bonferroni's multiple comparison test).

dynamic particle size (in aqueous media), while the TEM measures neat particle size (dry state).[42]

2.7. Nuclear Magnetic Resonance Spectroscopy. Micelle formation was confirmed by using NMR spectroscopy. Soluplus and TPGS ^{1}H NMR spectra were recorded independently by dissolving them in DMSO-d_6. The NMR spectra of B6 micelles prepared in deuterated water (D$_2$O) were then recorded. Figure 4 depicts representative NMR spectra of Soluplus, TPGS, and B6 micelle. The ^{1}H NMR spectra of Soluplus and TPGS were aligned with their respective chemical structures as shown in Figure 4. Along with their chemical structure, the matching ^{1}H NMR peak is assigned in their individual ^{1}H NMR spectra. The ^{1}H NMR peak assignments of Soluplus[43] and TPGS[44] were compared to the published literature to validate their accuracy. The hydrophilic and hydrophobic segments of Soluplus and TPGS were shaded blue and yellow, respectively, within their chemical structure.

The ^{1}H NMR peaks of their hydrophobic segments were distinctly visible in their respective NMR spectra (Figure 4). The same peaks had nearly disappeared in the NMR spectra of mixed micelles, where only the peak of PEG was present. A plausible explanation for this is the formation of micelles (core/shell structure). During micelle formation, the hydro-

phobic segments construct the micellar core, while the hydrophilic segment forms the shell of the micelles. Due to the core/shell structure of micelles, the protons associated with core forming segments make them less prone to diffuse. As a result, either the peak broadens (due to very slow diffusion) or disappears. A similar phenomenon was reported previously by Wu et al.[45], where the hydrophilic segments have comparatively less restrictions. Thus, their peaks were clearly visible, even after micelle formation. To get all potential ^{1}H NMR peaks, the NMR spectra of Soluplus and TPGS were recorded in DMSO-d_6. While the ^{1}H NMR spectrum of mixed micelles was recorded in D$_2$O to avoid any disassembly of micelles.

2.8. Micelle Stability Studies. Formulation F6 was freshly prepared and separated into two groups based on storage conditions. These groups were further subdivided into aliquots based on the sampling time points. One group was kept at room temperature, while the other was held at 4 °C. The results showed that mixed micelles F6 were stable under both storage conditions, with very minor changes in the size and PDI. As seen in Table 5, the changes were insignificant. At both conditions, the EE% did not change considerably after 15 days of storage. The EE% of F6 changed to 95.41 ± 2.10% and 95.21 ± 3.24% on day 15 of storage at ambient temperature and 4 °C, respectively, compared to day 0 (96.21 ± 1.44%).

Although the statistical analysis revealed that for days 5, 10, and 15, the increases in zeta potential values were significant ($p < 0.05$) when compared to day 0, the changes in the values were negligible (Table 5) In fact, the alterations were not significant enough to have an impact on the stability of micelles (i.e., no evidence of aggregation). On day 15 of storage at ambient temperature and 4 °C, the zeta potential changed to -1.23 ± 0.34 and -1.37 ± 0.39 mV, respectively, as compared to day 0 (-0.91 ± 0.10 mV).

2.9. Cellular Uptake Study. The therapeutic efficacy of nanoformulations is largely assessed by drug accumulation in target cells. The accumulation is mainly dependent upon the extent of cellular uptake and distribution properties of nanoformulations.[46] Previous reports have shown that nanoformulations decorated with TPGS have a high cellular uptake via a receptor-mediated active targeting mechanism.[47] In the current study, the cellular uptake capability of mixed micelles F6 (Soluplus: TPGS; 4:1) by A549 cells was evaluated using a fluorescent microscope operating in the fluorescence mode. The C-6-loaded mixed micelles were prepared with the same composition as that of F6, with the exception that BGT was replaced with C-6.

C-6 is a hydrophobic fluorescent dye that is utilized as a drug substitute in the investigations of nanoparticle uptake, particularly in micelles. It is a small molecule that can be internalized by cells through a variety of mechanisms, including passive diffusion and endocytosis. C-6 is a very stable dye with a high molar extinction coefficient and quantum yield. These characteristics render it an excellent probe for imaging.[48] Thus, C-6 was utilized as a substitute for BGT to evaluate the cellular uptake potential of mixed micelles.

In separate wells, A549 cells were incubated with free C-6 or C-6-loaded mixed micelles for 2 and 5 h. The fluorescence images of both treatment groups are presented in Figure 5A

and their respective fluorescence intensities were measured with the aid of ImageJ software. The apparent differences in the C-6 uptake after 2 and 5 h of incubation were depicted in Figure 5B,C, respectively. The comparison of free C-6 and C-6-loaded mixed micelle treatment groups revealed significant variations in the uptake. Following 2 and 5 h of exposure, the cells cultured with C-6-loaded mixed micelles exhibited 2.0 and 1.5 times ($p < 0.05$) higher fluorescence intensity than those cultured with free C-6. An increase in fluorescent intensity is confirming the increased cellular uptake in mixed micelle treated group. The increased levels of the fluorescence intensities may be attributed to the presence of TPGS in the mixed micelles, which works as an efflux transport inhibitor. Indeed, Tsai et al. discovered that TPGS-coated nanoparticles had more internalization in the resistant A549 cell lines, which might be attributed to the presence of TPGS.[49] Furthermore, Cheng et. al also reported increased uptake of TPGS functionalized mesoporous silica nanoparticles loaded with doxorubicin in the A549 and MDR A549 cell lines.[50]

2.10. In Vitro Cytotoxicity Study. MTT assay was used to determine the antiproliferative effect of free BGT, empty mixed micelles (B6), and BGT-loaded mixed micelles (F6) on A549 cell lines. The B6 micelles had no apparent detrimental impact on the survival of A549 cells up to a concentration of 12.5 μg/mL after 24 h of incubation. At B6 concentrations $\leq$25 μg/mL, it caused cytotoxicity in the A549 cell line that was significantly different from the control group ($p < 0.05$). After incubation with 100 μg/mL of B6 for 24 h, only $44.32 \pm 2.10\%$ remained viable. A plausible explanation for the cytotoxicity of B6 micelles is the presence of TPGS in the micelles. It has been reported that TPGS induces apoptosis, which could be the possible reason for the cytotoxicity of B6 micelles against A549 cells at higher concentrations.[51] The IC$_{50}$ value for B6 micelles was found to be 98.32 ± 7.22 μg/mL (Table 6) after 24 h of exposure. Figure 6 shows the in

Table 6. IC$_{50}$ (Mean $\pm$ SD) Values of Free BGT, Blank Micelles (B6) and Mixed Micelles (F6) Against A549 Cell Lines After Incubation for 24 h

	BGT	B6	F6
IC$_{50}$ (μg/mL)	61.45 ± 6.349	98.32 ± 7.215^a	22.59 ± 6.07^{ab}

$^a p < 0.05$ versus BGT. $^b p < 0.05$ versus F6.

vitro cytotoxic effects of free BGT, B6, and F6 micelles against the control group. F6 mixed micelles produced encouraging results, as evidenced by a significant ($p < 0.05$) decrease in IC$_{50}$ values for BGT-loaded mixed micelles (22.59 ± 6.07 μg/mL) as compared to BGT-free drug (61.45 ± 6.349 μg/mL). After 24 h of incubation, the IC$_{50}$ values of F6 micelles in the A549 cell line were nearly three times lower than that of free BGT. The results of the present research clearly demonstrate that BGT-loaded mixed micelles had a greater anticancer activity against A549 cell lines compared to free BGT after 24 h of incubation. The enhanced cytotoxicity of BGT-loaded mixed micelles relative to free BGT could be attributed to the carrier's nanoscale size, enhanced encapsulation, as well as the presence of TPGS.[52] The confirmation of P-gp expression and function in A549 cell monolayers was already reported.[53−56] TPGS is a well-known P-gp inhibitor. It is reported to reduce P-gp ATPase activity by blocking ATP binding sites, hence decreasing P-gp-mediated efflux, resulting in improved drug accumulation in cells.[57]
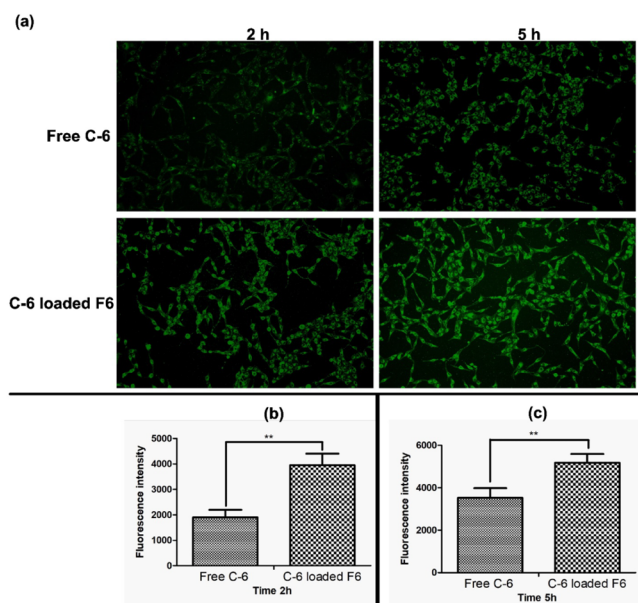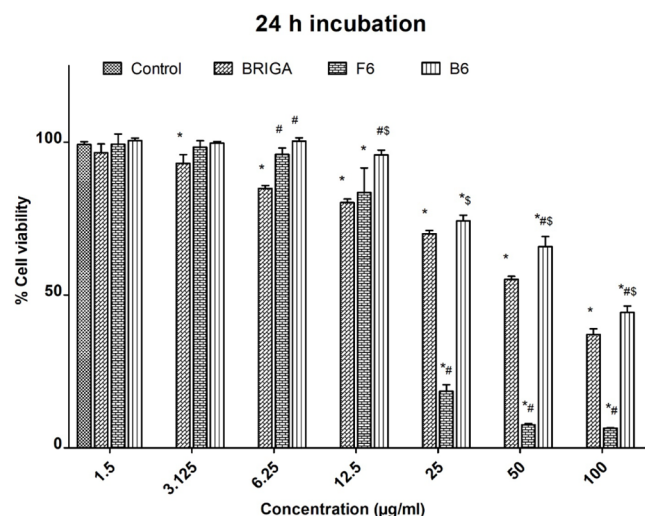

Figure 5. In vitro cellular uptake in A549 cells. (a). Green fluorescence images after 2 and 5 h of incubation with free Coumarin 6 (C-6) and C-6 encapsulated F6 at 37 °C. (b) Quantitative fluorescence uptake after 2h and, (c) Quantitative fluorescence uptake after 5h ** $p < 0.05$ free C-6 versus C-6-loaded F6 after 2 and 5 h of incubation.

Figure 6. In vitro cell viability of A549 cells after incubation with different concentrations of free BGT and BGT-loaded F6 mixed micelles for 24 h * $p < 0.05$ versus control untreated cells after 24 h incubation # $p < 0.05$ versus free BGT after 24 h of incubation. $ $p < 0.05$ versus F6 after 24 h of incubation.

3. CONCLUSIONS

The thin film hydration method was successfully employed for the preparation of BGT-loaded Soluplus/TPGS mixed micelles. The mixed micelles appeared as a viable strategy for improving BGT solubility, stability, and delivery efficiency. BGT solubility was raised approximately 10 times with the help of mixed micelles. Formulation prepared with Soluplus: TPGS at a ratio of 4:1 showed the desired particle size and encapsulation efficiency. The results of cellular uptake and cytotoxicity studies showed a clear advantage of using mixed micelles for BGT delivery as opposed to free drug. Our research work presented here showed that the developed Soluplus/TPGS mixed micelles have a great deal of potential for use as a BGT delivery system in the treatment of lung cancer.

4. MATERIALS AND METHODS

4.1. Materials. Brigatinib (BGT) was purchased from Beijing Mesochem Technology Co. Ltd. (Beijing China). Soluplus was procured from BASF Pharma (New Jersey, USA). TPGS, DMSO-d_6, D$_2$O, ethanol, methanol, acetonitrile and coumarin-6 were purchased from Sigma-Aldrich (St. Louis, USA). Milli-Q water was prepared in-house using a Merck Milli-Q Millipore ultrapure water purification system. Dulbecco's Modified Eagle Medium (DMEM) was purchased from Life Technologies Ltd. (Paisley, UK).

4.2. Methods. *4.2.1. Preparation of BGT-Loaded Single and Mixed Micelles.* The thin film hydration method was employed to prepare BGT-loaded Soluplus/TPGS mixed micelles. Briefly, 5 mg of BGT was dissolved in 5 mL of anhydrous ethanol by vortex-mixing and heating in a water bath (set at 50 °C). Once the BGT has been completely dissolved, Soluplus: TPGS at different ratios (1:4, 2:3, 1:1, 3:2, and 4:1), representing 1.6% w/v of total polymer concentration, were added independently to the ethanolic solution of BGT and mixed until a clear solution was achieved. The solvent was then evaporated with the aid of a rotary evaporator at 40 °C under reduced pressure and allowed to form a thin film. The thin-film-containing round-bottomed flask was then

maintained overnight in a vacuum oven at 40 °C to eliminate any remaining ethanol. The dried film was then hydrated with 5 mL of water for 30 min to yield the micelles. After the hydration process, the micellar dispersion was centrifuged at 13 500 rpm for 5 min to remove any unencapsulated BGT or precipitated polymer. The supernatant containing BGT-loaded mixed micelles in liquid form was collected for further studies. Similarly, BGT-loaded single micelles of Soluplus and TPGS with 1.6% (w/v) polymer concentration were also prepared. The blank single and mixed micelles were also prepared in a similar manner but without adding the drug.

4.2.2. Determination of Critical Micelle Concentration (CMC). Dynamic light scattering method was used to calculate the CMC values of the prepared micelles in aqueous solution.[37] All measurements were performed at a scattering angle of 173° to the incident beam. Blank micelles were prepared and further diluted in the range from 2000 to 0.1 μg/ mL using Milli-Q water. The prepared micellar dispersions were equilibrated overnight at room temperature prior to analysis. A graph between polymer concentration (μg/mL) versus the derived count rates plotted on the X and Y axis, respectively. The copolymer concentration that was associated with an abrupt increase in the scattering intensity was considered the CMC value. Mathematically, the point of intersection of two straight lines was calculated using the following equation

$$\text{Point of intersection at } X \text{ axis} = \frac{C_2 - C_1}{M_1 - M_2}$$

Where C_1 and C_2 are the intercept values of the trend line eqs 1 and 2, respectively, and M_1 and M_2 are the slope values of those two trend line eqs 1 and 2, respectively.

4.2.3. Measurement of Micellar Size, Polydispersity Index (PDI), and Zeta Potential. The hydrodynamic diameter and PDI of blank and BGT-loaded micelles were measured using a Zetasizer NanoZS (Malvern Instrument Ltd., Malvern, UK) instrument. Deionized water was used as the dispersion medium for all of the prepared micelles. Prior to analysis, the samples were equilibrated for 2 min at 25 °C. The measurements were performed using a noninvasive backscatter technique at 173° of detection angle. All measurements were performed in triplicate, and their mean as well as standard deviation (SD) values were reported.

4.2.4. Estimation of Encapsulation Efficiency (EE%) and Drug Loading (DL%). BGT-loaded micelles were diluted ten times in methanol and aggressively vortexed to rupture the micelles and release the BGT. A previously reported high-performance liquid chromatography (HPLC) method was used to estimate the quantity of BGT.[58] The HPLC analysis was carried out on a Waters 1500 Series controller (Boston, MA, USA) equipped with a binary pump (Waters 1525, Boston, MA, USA), a dual wavelength UV detector (Waters 2489, Boston, MA, USA), and an autosampler (Waters 2707, Boston, MA, USA). The HPLC system was monitored using Breeze (Waters, Boston, MA, USA), an automated system performance monitoring software. The BGT was separated using a C$_{18}$ column (Macherey-Nagel 4.6 × 150 mm, 5 μm particle size) as the stationary phase, while methanol:milli-Q water (75:25 v/v) served as the mobile phase. The flow rate was set at 1 mL/min, and detection was carried out at 283 nm at room temperature. Equations 1 and 2 we re used to calculate the EE% and DL% of BGT in different micelles, respectively:

$$EE\% = \frac{m_{\text{BGT,loaded}}}{m_{\text{BGT,added}}} \times 100 \tag{1}$$

$$DL\% = \frac{m_{\text{BGT,loaded}}}{m_{\text{Soluplus}} + m_{\text{TPGS}} + m_{\text{BGT,added}}} \times 100 \tag{2}$$

where $m_{\text{BGT,loaded}}$ is the mass of BGT loaded, $m_{\text{BGT,added}}$ is the mass of BGT added, m_{Soluplus} is the mass of Soluplus, and m_{TPGS} is the mass of TPGS. All measurements were performed in triplicate, and results were expressed as mean ± SD.

4.2.5. In Vitro Release Profile of BGT from Mixed Micelle. In vitro release of BGT from the BGT ethanolic solution and mixed micellar systems (with EE% more than 90%) was performed by applying the dialysis method. The volumes equivalent to 1500 μg of BGT were placed into dialysis bags (molecular weight cut off = 14 kDa) and subsequently put into 100 mL of phosphate-buffered saline (PBS, pH 7.4) containing 0.5% v/v Tween 80 (to obtain sink condition). The samples were incubated in a shaking water bath SW22 (Julabo, Seelbach, Germany) set at 50 rpm and maintained at 37 °C. One mL of the release media was withdrawn and replaced with 1 mL of fresh media at predefined time intervals (0.25, 0.5, 1, 2, 4, 6, 9, 12, 24, 48, and 72 h). The collected samples were analyzed by the previously mentioned HPLC method to quantify the released BGT.

4.2.6. Morphological Examination of Micelles. The TEM technique was used to examine the morphology of the micelles. The micelles were diluted 100 times with Milli-Q water before being drop cast on a carbon Type-B copper grid (Ted Pella Inc., Redding, CA, USA). The negative staining of the drop-casted micelles was performed by adding 1% solution of phosphotungstic acid in PBS (pH = 7.0). After drying at room temperature in a desiccator, the grids were loaded into the JEM-1010 TEM (JEOL, Tokyo, Japan) operating at an accelerating voltage of 80 kV. The images were captured with a high-speed readout side-mounted MegaViewG2 camera (Olympus, Hamburg, Germany) and processed with the iTEM software (Olympus Soft Imaging Solutions GmbH, Münster, Germany).

4.2.7. Nuclear Magnetic Resonance (NMR) Spectroscopy. ^{1}H NMR spectra of Soluplus, TPGS, and their prepared micelles were acquired by a Bruker AVANCE NMR spectrometer operating at 400 MHz. Spectra were referenced using the spectrometer default residual protonated solvent as an internal reference. Samples of Soluplus and TPGS were prepared in DMSO-d_6, while the micelles were prepared as described in section 3.2.1, except that Milli-Q water was replaced with D$_2$O. All NMR spectra were processed using the online NMR spectra processing software NMRium (Zakodium Sàrl, Lonay, Switzerland).

4.2.8. Micelle Stability Studies. The prepared mixed micelles were stored at room temperature or 4 °C for 15 days. The micelle size, PDI, zeta potential, and EE% were measured on days 5, 10, and 15 after incubation.

4.2.9. Cell Culture Model. The human lung cancer cells (A549) were grown at 37 °C in a humidified incubator with a 5% CO$_2$ environment in Dulbecco's minimal essential medium (DMEM) supplemented with 10% fetal bovine serum (FBS, Life Technologies Ltd. UK) and 1% penicillin-streptomycin solution (M&C Gene Technology Co. Ltd.). After achieving approximately 80% confluency, the cells were harvested using 0.25% trypsin containing EDTA and phenol red. The harvested cells were further seeded in 96- and 6-well plates

for conducting cell viability and cellular uptake experiments, respectively.

4.2.10. Cellular Uptake Study. Coumarin-6 (C-6) was employed as a fluorescent probe and encapsulated in selected mixed micelles in place of BGT to assess cellular uptake in A549 cell lines. Briefly, the cells were seeded in six-well plates (Corning Costar, Fisher Scientific, USA) at a density of 5 × 10^5 cells/well and incubated for 24 h. After 24 h, the cell culture media was removed and fresh medium containing 1 μg/mL of free C-6 or C-6-loaded mixed micelles was added in the designated wells. After 2 and 5 h of incubation, the media was meticulously removed, and the cell layers were washed thrice with sterile PBS. The cells were then fixed with 4% paraformaldehyde for 10 min before being examined under a fluorescent microscope (OPTIKA Microscopes, Italy) and the fluorescent images were captured. The fluorescence intensities were measured with the aid of the software ImageJ (version 1.54d, National Institute of Health, USA).[38]

4.2.11. In Vitro Cytotoxicity Study. MTT assay was used to assess the cytotoxicity of blank Soluplus/TPGS mixed micelles, free BGT, and selected BGT-loaded Soluplus/TPGS mixed micelles in A549 cell lines under aseptic conditions. In brief, 1.5 × 10^4 cells per well were seeded into 96-well plates with DMEM containing 10% FBS and allowed to adhere to the wells overnight at 37 °C temperature and 5% CO$_2$ in an incubator. The stock of free BGT was prepared in a mixture of 10.0% DMSO and 7.0% Tween 80 in water and then further diluted with the culture media to make the DMSO concentration less than 0.5% for all treatments. The adhered cells were then cocultured in triplicate with blank Soluplus/TPGS mixed micelles, various concentrations of free BGT, and selected BGT-loaded mixed micelles. After 24 h of incubation, the medium of 96-well plates was replaced with fresh medium. Following that, 50 μL of MTT solution (2 mg/mL in PBS) was poured into each well and incubated for a further 4 h. The contents of the wells were then removed, and 25 μL of Sorensen's glycine buffer and 200 μL of DMSO were added. To assess cell viability, the absorbance of each well was measured at 490 nm by using a BioTek synergy HT microplate reader (BioTek Instruments, Inc., Winooski, USA). The untreated cells served as the negative control, while DMSO served as blank. Cell viability was determined as a percentage of absorbance compared to a 100% negative control.

4.2.12. Data Analysis. All data were provided as mean ± SD. Statistical significance was determined using either the Student's *t*-test or a one-way analysis of variance (ANOVA) followed by Bonferroni's multiple comparison test, depending on the number of groups being compared. The level of significance was set at $p < 0.05$.

■ AUTHOR INFORMATION

Corresponding Author

Ziyad Binkhathlan — *Department of Pharmaceutics, College of Pharmacy, King Saud University, Riyadh 11451, Saudi Arabia;* ◉ orcid.org/0000-0003-1853-7490; Email: zbinkhathlan@ksu.edu.sa

Authors

Raisuddin Ali — *Department of Pharmaceutics, College of Pharmacy, King Saud University, Riyadh 11451, Saudi Arabia;* ◉ orcid.org/0000-0001-9892-2158

Wajhul Qamar − *Department of Pharmaceutics, College of Pharmacy, King Saud University, Riyadh 11451, Saudi Arabia*

Mohd Abul Kalam − *Department of Pharmacology and Toxicology, College of Pharmacy, King Saud University, Riyadh 11451, Saudi Arabia;* ⊙ orcid.org/0000-0002-5713-8858

Complete contact information is available at:
https://pubs.acs.org/10.1021/acsomega.4c06264

Funding

Notes

The authors declare no competing financial interest.

■ REFERENCES

(1) Wu, S.; Powers, S.; Zhu, W.; Hannun, Y. A. Substantial Contribution of Extrinsic Risk Factors to Cancer Development. *Nature* **2016**, *529*, 43−47.

(2) Sung, H.; Ferlay, J.; Siegel, R. L.; Laversanne, M.; Soerjomataram, I.; Jemal, A.; Bray, F. Global Cancer Statistics 2020: GLOBOCAN Estimates of Incidence and Mortality Worldwide for 36 Cancers in 185 Countries. *Ca-Cancer J. Clin.* **2021**, *71*, 209−249.

(3) Gee, K.; Yendamuri, S. Lung Cancer in Females-Sex-Based Differences from Males in Epidemiology, Biology, and Outcomes: A Narrative Review. *Transl. Lung Cancer Res.* **2024**, *13*, 163−178.

(4) Fujimoto, J.; Wistuba, I. I. Current Concepts on the Molecular Pathology of Non-Small Cell Lung Carcinoma. *Semin. Diagn. Pathol.* **2014**, *31*, 306−313.

(5) Villalobos, P.; Wistuba, I. I. Lung Cancer Biomarkers. *Hematol. Oncol. Clin. North. Am.* **2017**, *31*, 13−29.

(6) Huang, W.-S.; Liu, S.; Zou, D.; Thomas, M.; Wang, Y.; Zhou, T.; Romero, J.; Kohlmann, A.; Li, F.; Qi, J.; et al. Discovery of Brigatinib (AP26113), a Phosphine Oxide-Containing, Potent, Orally Active Inhibitor of Anaplastic Lymphoma Kinase. *J. Med. Chem.* **2016**, *59*, 4948−4964.

(7) Sabari, J. K.; Santini, F.; Schram, A. M.; Bergagnini, I.; Chen, R.; Mrad, C.; Lai, W. V.; Arbour, K. C.; Drilon, A. The Activity, Safety, and Evolving Role of Brigatinib in Patients with ALK-Rearranged Non-Small Cell Lung Cancers. *OncoTargets Ther.* **2017**, *10*, 1983−1992.

(8) Su, M.; Tian, H.; Zhou, L.; Li, Q.; Wang, S.; Haung, C.; Nice, E. C.; Zheng, S.; Li, J. Brigatinib-Repurposed Chemo-Photodynamic Therapy Nanoplatform via Effective Apoptosis against Colorectal Cancer. *Mater. Des.* **2023**, *226*, 111613.

(9) Mohammad, M.; Anwer, M. K.; Fatima, F.; Alshahrani, S. M.; Alshetaili, A. S.; Alalaiwe, A.; Alsulays, B. B.; Shakeel, F. Temperature Dependent Solubility Studies of Brigatinib in Some Pure Solvents Useful in Dosage Form Development. *Acta Polym. Pharm.-Drug Res.* **2019**, *76*, 225−232.

(10) Gupta, N.; Hanley, M. J.; Griffin, R. J.; Zhang, P.; Venkatakrishnan, K.; Sinha, V. Clinical Pharmacology of Brigatinib: A Next-Generation Anaplastic Lymphoma Kinase Inhibitor. *Clin. Pharmacokinet.* **2023**, *62*, 1063−1079.

(11) *Alunbrig-Epar-Public-Assessment-Report_en* https://www.ema. europa.eu/en/documents/assessment-report/alunbrig-epar-public-assessment-report_en.pdf. (Accessed on 11 January 2023).

(12) Altamimi, M. A.; Hussain, A.; AlRajhi, M.; Alshehri, S.; Imam, S. S.; Qamar, W. Luteolin-Loaded Elastic Liposomes for Transdermal Delivery to Control Breast Cancer: In Vitro and Ex Vivo Evaluations. *Pharmaceuticals* **2021**, *14*, 1143.

(13) Alsulays, B. B.; Anwer, M. K.; Soliman, G. A.; Alshehri, S. M.; Khafagy, E.-S. Impact Of Penetratin Stereochemistry On The Oral Bioavailability Of Insulin-Loaded Solid Lipid Nanoparticles. *Int. J. Nanomed.* **2019**, *14*, 9127−9138.

(14) Jamil, A.; Aamir Mirza, M.; Anwer, M. K.; Thakur, P. S.; Alshahrani, S. M.; Alshetaili, A. S.; Telegaonkar, S.; Panda, A. K.; Iqbal, Z. Co-Delivery of Gemcitabine and Simvastatin through PLGA Polymeric Nanoparticles for the Treatment of Pancreatic Cancer: *In-Vitro* Characterization, Cellular Uptake, and Pharmacokinetic Studies. *Drug Dev. Ind. Pharm.* **2019**, *45*, 745−753.

(15) Zaki, R. M.; Alfadhel, M. M.; Alshahrani, S. M.; Alsaqr, A.; Al-Kharashi, L. A.; Anwer, M. K. Formulation of Chitosan-Coated Brigatinib Nanospanlastics: Optimization, Characterization, Stability Assessment and In-Vitro Cytotoxicity Activity against H-1975 Cell Lines. *Pharmaceuticals* **2022**, *15*, 348.

(16) Ahmed, M. M.; Fatima, F.; Anwer, M. K.; Aldawsari, M. F.; Alsaidan, Y. S. M.; Alfaiz, S. A.; Haque, A.; Az, A.; Alhazzani, K. Development and Characterization of Brigatinib Loaded Solid Lipid Nanoparticles: In-Vitro Cytotoxicity against Human Carcinoma A549 Lung Cell Lines. *Chem. Phys. Lipids* **2020**, *233*, 105003.

(17) Ansari, M. J.; Alnakhli, M.; Al-Otaibi, T.; Meananzel, O. A.; Anwer, M. K.; Ahmed, M. M.; Alshahrani, S. M.; Alshetaili, A.; Aldawsari, M. F.; Alalaiwe, A. S.; et al. Formulation and Evaluation of Self-Nanoemulsifying Drug Delivery System of Brigatinib: Improvement of Solubility, in Vitro Release, Ex-Vivo Permeation and Anticancer Activity. *J. Drug Delivery Sci. Technol.* **2021**, *61*, 102204.

(18) Ahmed, M. M.; Fatima, F.; Anwer, M. K.; Aldawsari, M. F.; Bhatia, S.; Al-Harrasi, A. Brigatinib Loaded Poly(d,l-Lactide-Co-Glycolide) Nanoparticles for Improved Anti-Tumoral Activity against Non-Small Cell Lung Cancer Cell Lines. *Drug Dev. Ind. Pharm.* **2021**, *47*, 1112−1120.

(19) Chiappetta, D. A.; Sosnik, A. Poly(Ethylene Oxide)−Poly-(Propylene Oxide) Block Copolymer Micelles as Drug Delivery Agents: Improved Hydrosolubility, Stability and Bioavailability of Drugs. *Eur. J. Pharm. Biopharm.* **2007**, *66*, 303−317.

(20) Manjappa, A. S.; Kumbhar, P. S.; Patil, A. B.; Disouza, J. I.; Patravale, V. B. Polymeric Mixed Micelles: Improving the Anticancer Efficacy of Single-Copolymer Micelles. *Crit. Rev. Ther. Drug Carrier Syst* **2019**, *36*, 1−58.

(21) Cagel, M.; Tesan, F. C.; Bernabeu, E.; Salgueiro, M. J.; Zubillaga, M. B.; Moretton, M. A.; Chiappetta, D. A. Polymeric Mixed Micelles as Nanomedicines: Achievements and Perspectives. *Eur. J. Pharm. Biopharm.* **2017**, *113*, 211−228.

(22) Lohan, S.; Sharma, T.; Saini, S.; Swami, R.; Dhull, D.; Beg, S.; Raza, K.; Kumar, A.; Singh, B. QbD-Steered Development of Mixed Nanomicelles of Galantamine: Demonstration of Enhanced Brain Uptake, Prolonged Systemic Retention and Improved Biopharmaceutical Attributes. *Int. J. Pharm.* **2021**, *600*, 120482.

(23) Cabral, H.; Miyata, K.; Osada, K.; Kataoka, K. Block Copolymer Micelles in Nanomedicine Applications. *Chem. Rev.* **2018**, *118*, 6844−6892.

(24) Varela-Garcia, A.; Concheiro, A.; Alvarez-Lorenzo, C. Soluplus Micelles for Acyclovir Ocular Delivery: Formulation and Cornea and Sclera Permeability. *Int. J. Pharm.* **2018**, *552*, 39−47.

(25) Zeng, Y.-C.; Li, S.; Liu, C.; Gong, T.; Sun, X.; Fu, Y.; Zhang, Z.-R. Soluplus Micelles for Improving the Oral Bioavailability of Scopoletin and Their Hypouricemic Effect in Vivo. *Acta Pharmacol. Sin.* **2017**, *38*, 424−433.

(26) Jin, I. S.; Jo, M. J.; Park, C.-W.; Chung, Y. B.; Kim, J.-S.; Shin, D. H. Physicochemical, Pharmacokinetic, and Toxicity Evaluation of Soluplus® Polymeric Micelles Encapsulating Fenbendazole. *Pharmaceutics* **2020**, *12*, 1000.

(27) Xia, D.; Yu, H.; Tao, J.; Zeng, J.; Zhu, Q.; Zhu, C.; Gan, Y. Supersaturated Polymeric Micelles for Oral Cyclosporine A Delivery: The Role of Soluplus-Sodium Dodecyl Sulfate Complex. *Colloids Surf., B* **2016**, *141*, 301−310.

(28) Bernabeu, E.; Gonzalez, L.; Cagel, M.; Gergic, E. P.; Moretton, M. A.; Chiappetta, D. A. Novel Soluplus(®)-TPGS Mixed Micelles for Encapsulation of Paclitaxel with Enhanced in Vitro Cytotoxicity on Breast and Ovarian Cancer Cell Lines. *Colloids Surf., B* **2016**, *140*, 403−411.

(29) Yang, C.; Wu, T.; Qi, Y.; Zhang, Z. Recent Advances in the Application of Vitamin E TPGS for Drug Delivery. *Theranostics* **2018**, *8*, 464−485.

(30) Guo, Y.; Luo, J.; Tan, S.; Otieno, B. O.; Zhang, Z. The Applications of Vitamin E TPGS in Drug Delivery. *Eur. J. Pharm. Sci. Off. J. Eur. Fed. Pharm. Sci.* **2013**, *49*, 175−186.

(31) Bogman, K.; Erne-Brand, F.; Alsenz, J.; Drewe, J. The Role of Surfactants in the Reversal of Active Transport Mediated by Multidrug Resistance Proteins. *J. Pharm. Sci.* **2003**, *92*, 1250−1261.

(32) Pignatello, R.; Corsaro, R.; Bonaccorso, A.; Zingale, E.; Carbone, C.; Musumeci, T. Soluplus® Polymeric Nanomicelles Improve Solubility of BCS-Class II Drugs. *Drug Delivery Transl. Res.* **2022**, *12*, 1991−2006.

(33) Mahajan, H. S.; Patil, P. H. Central Composite Design-Based Optimization of Lopinavir Vitamin E-TPGS Micelle: In Vitro Characterization and in Vivo Pharmacokinetic Study. *Colloids Surf., B* **2020**, *194*, 111149.

(34) U.S. Pharmacopeial Convention. *Council of Experts and its Expert Committees Usp39-Nf34*; The United States Pharmacopoeia; United States Pharmacopeia, 2015. ISBN 978−1-936424−44−3

(35) Piazzini, V.; Landucci, E.; Urru, M.; Chiarugi, A.; Pellegrini-Giampietro, D. E.; Bilia, A. R.; Bergonzi, M. C. Enhanced Dissolution, Permeation and Oral Bioavailability of Aripiprazole Mixed Micelles: In Vitro and in Vivo Evaluation. *Int. J. Pharm.* **2020**, *583*, 119361.

(36) Topel, Ö.; Çakır, B. A.; Budama, L.; Hoda, N. Determination of Critical Micelle Concentration of Polybutadiene-Block-Poly-(Ethyleneoxide) Diblock Copolymer by Fluorescence Spectroscopy and Dynamic Light Scattering. *J. Mol. Liq.* **2013**, *177*, 40−43.

(37) Cagel, M.; Bernabeu, E.; Gonzalez, L.; Lagomarsino, E.; Zubillaga, M.; Moretton, M. A.; Chiappetta, D. A. Mixed Micelles for Encapsulation of Doxorubicin with Enhanced in Vitro Cytotoxicity on Breast and Ovarian Cancer Cell Lines versus Doxil®. *Biomed. Pharmacother.* **2017**, *95*, 894−903.

(38) Alshetaili, A. S.; Ali, R.; Qamar, W.; Almohizea, S.; Anwer, M. K. Preparation, Optimization, and Characterization of Chrysin-Loaded TPGS-b-PCL Micelles and Assessment of Their Cytotoxic Potential in Human Liver Cancer (Hep G2) Cell Lines. *Int. J. Biol. Macromol.* **2023**, *246*, 125679.

(39) Oerlemans, C.; Bult, W.; Bos, M.; Storm, G.; Nijsen, J. F. W.; Hennink, W. E. Polymeric Micelles in Anticancer Therapy: Targeting, Imaging and Triggered Release. *Pharm. Res.* **2010**, *27*, 2569−2589.

(40) Mehta, S. K.; Jindal, N. Mixed Micelles of Lecithin−Tyloxapol as Pharmaceutical Nanocarriers for Anti-Tubercular Drug Delivery. *Colloids Surf., B* **2013**, *110*, 419−425.

(41) Kobryń, J.; Sowa, S.; Gasztych, M.; Dryś, A.; Musiał, W. Influence of Hydrophilic Polymers on the *β* Factor in Weibull Equation Applied to the Release Kinetics of a Biologically Active Complex of *Aesculus Hippocastanum*. *Int. J. Polym. Sci.* **2017**, *2017*, 1−8.

(42) Souza, T. G. F.; Ciminelli, V. S. T.; Mohallem, N. D. S. A Comparison of TEM and DLS Methods to Characterize Size Distribution of Ceramic Nanoparticles. *J. Phys.: Conf. Ser.* **2016**, *733*, 012039.

(43) Sofroniou, C.; Baglioni, M.; Mamusa, M.; Resta, C.; Doutch, J.; Smets, J.; Baglioni, P. Self-Assembly of Soluplus in Aqueous Solutions: Characterization and Prospectives on Perfume Encapsulation. *ACS Appl. Mater. Interfaces* **2022**, *14*, 14791−14804.

(44) Dong, K.; Lei, Q.; Guo, R.; Wu, X.; Zhang, Y.; Cui, N.; Shi, J.; Lu, T. Regulating Intracellular ROS Signal by a Dual pH/Reducing-Responsive Nanogels System Promotes Tumor Cell Apoptosis. *Int. J. Nanomed.* **2019**, *14*, 5713−5728.

(45) Wu, L.; Lal, J.; Simon, K. A.; Burton, E. A.; Luk, Y.-Y. Nonamphiphilic Assembly in Water: Polymorphic Nature, Thread Structure, and Thermodynamic Incompatibility. *J. Am. Chem. Soc.* **2009**, *131*, 7430−7443.

(46) Mu, L.; Feng, S.-S. PLGA/TPGS Nanoparticles for Controlled Release of Paclitaxel: Effects of the Emulsifier and Drug Loading Ratio. *Pharm. Res.* **2003**, *20*, 1864−1872.

(47) Zhao, S.; Tan, S.; Guo, Y.; Huang, J.; Chu, M.; Liu, H.; Zhang, Z. pH-Sensitive Docetaxel-Loaded D-*α*-Tocopheryl Polyethylene Glycol Succinate−Poly(*β*-Amino Ester) Copolymer Nanoparticles for Overcoming Multidrug Resistance. *Biomacromolecules* **2013**, *14*, 2636−2646.

(48) Mei, L.; Zhang, H.; Zeng, X.; Huang, L.; Wang, Z.; Liu, G.; Wu, Y.; Yang, C. Fabrication of Genistein-Loaded Biodegradable TPGS-b-PCL Nanoparticles for Improved Therapeutic Effects in Cervical Cancer Cells. *Int. J. Nanomed.* **2015**, 2461.

(49) Tsai, H.-I.; Jiang, L.; Zeng, X.; Chen, H.; Li, Z.; Cheng, W.; Zhang, J.; Pan, J.; Wan, D.; Gao, L.; et al. DACHPt-Loaded Nanoparticles Self-Assembled from Biodegradable Dendritic Copolymer Polyglutamic Acid-b-D-*α*-Tocopheryl Polyethylene Glycol 1000 Succinate for Multidrug Resistant Lung Cancer Therapy. *Front. Pharmacol.* **2018**, *9*, 119.

(50) Cheng, W.; Liang, C.; Xu, L.; Liu, G.; Gao, N.; Tao, W.; Luo, L.; Zuo, Y.; Wang, X.; Zhang, X.; et al. TPGS-Functionalized Polydopamine-Modified Mesoporous Silica as Drug Nanocarriers for Enhanced Lung Cancer Chemotherapy against Multidrug Resistance. *Small* **2017**, *13*, 1700623.

(51) Tang, L.; Huang, K.; Jiang, W.; Fu, L.; Zhang, R.; Shen, L.; Ou, Z.; Huang, Y.; Zhang, Z. Exploration of the Inhibition Action of TPGS on Tumor Cells and Its Combined Use with Chemotherapy Drugs. *Drug Delivery* **2023**, *30*, 2183830.

(52) Ding, Y.; Wang, C.; Wang, Y.; Xu, Y.; Zhao, J.; Gao, M.; Ding, Y.; Peng, J.; Li, L. Development and Evaluation of a Novel Drug Delivery: Soluplus®/TPGS Mixed Micelles Loaded with Piperine *in Vitro* and *in Vivo*. *Drug Dev. Ind. Pharm.* **2018**, *44*, 1409−1416.

(53) Bosquillon, C. Drug Transporters in the Lung—Do They Play a Role in the Biopharmaceutics of Inhaled Drugs? *J. Pharm. Sci.* **2010**, *99*, 2240−2255.

(54) Endter, S.; Becker, U.; Daum, N.; Huwer, H.; Lehr, C.-M.; Gumbleton, M.; Ehrhardt, C. P-Glycoprotein (MDR1) Functional Activity in Human Alveolar Epithelial Cell Monolayers. *Cell Tissue Res.* **2007**, *328*, 77−84.

(55) Salomon, J. J.; Ehrhardt, C. Nanoparticles Attenuate P-Glycoprotein/MDR1 Function in A549 Human Alveolar Epithelial Cells. *Eur. J. Pharm. Biopharm.* **2011**, *77*, 392−397.

(56) Takano, M.; Higa, S.; Furuichi, Y.; Naka, R.; Yumoto, R. Suppression of P-Glycoprotein by Cigarette Smoke Extract in Human Lung-Derived A549/P-Gp Cells. *Drug Metab. Pharmacokinet.* **2020**, *35*, 214−219.

(57) Liu, T.; Liu, X.; Xiong, H.; Xu, C.; Yao, J.; Zhu, X.; Zhou, J.; Yao, J. Mechanisms of TPGS and Its Derivatives Inhibiting P-Glycoprotein Efflux Pump and Application for Reversing Multidrug Resistance in Hepatocellular Carcinoma. *Polym. Chem.* **2018**, *9*, 1827−1839.

(58) Akter, M. R.; Hossain, M. S.; Khairul Alam, K. M.; Rafiquzzaman, M. Development and Validation of RP-HPLC Method for the Determination of Anticancer Drug Brigatinib. *GSC Biol. Pharm. Sci.* **2023**, *23*, 030−041.